International Conference on Applied Energy 2019
Aug 12-15, 2019, Västerås, Sweden
Paper ID: 1060

EMPIRICAL MODELLING OF PRESSURE DROP IN GAS CHANNELS OF POLYMER ELECTROLYTE FUEL CELLS

Zan Wu

Department of Energy Sciences, Lund University, Lund, Sweden

ABSTRACT

The frictional pressure drop characteristics in gas channels of Polymer Electrolyte Fuel Cells (PEFCs) are modelled in this work. The two-phase flow in gas channels of PEFCs has its special features: (1) combination of reactant gas, water vapor and liquid water, (2) flow in micro/minichannels, (3) reactant consumption, (4) condensation from water vapor, (5) continuous water introduction from reaction and (6) flow pattern transitions. Therefore, previous two-phase pressure drop correlations, primarily for adiabatic gas-liquid flow, might not be able to capture the pressure drop in the gas channel with a porous wall. The new flow-pattern based pressure drop method covers three major flow regimes in gas channels, i.e., the single-phase gas flow zone, and droplet/mist flow and slug/film flow in the two-phase flow zone. In the droplet/mist flow regime, a homogeneous flow modelling was adopted, while in the slug/film flow regime, a modified Chisholm value of 8.5 was used. The new predictive tool presents improved accuracy in pressure drop estimation for different current densities and stoichiometric ratios of operating PEFCs.

Keywords: Pressure drop, two-phase flow, polymer electrolyte fuel cell, flow pattern, slug/film flow

NONMENCLATURE

A_c	cross-section area, m^2
A_{em}	Effective membrane area, m^2
C	Chisholm parameter
D_h	hydraulic diameter, m
F	Faraday's constant, C mol^{-1}
f	friction factor
G	mass flux, kg m^{-2} s^{-1}
i	current density, A m^{-2}
j	superficial velocity, m s^{-1}
L	length, m
M	molecular weight, kg mol^{-1}
$\dot{m}$	mass flow rate, kg s^{-1}
N	number of channels
n	number of moles, mol
P	pressure, Pa
Re	Reynolds number
RH	relative humidity
T	temperature, K
X	Martinelli parameter
x	gas flow quality
z	position
Greek symbols	
ΔP	pressure drop, Pa
Φ^2	two-phase frictional multiplier
α	aspect ratio
β	net water flux per proton flux
ζ	gas flow stoichiometry
μ	viscosity, Pa s
ρ	density, kg m^{-3}
ω	interaction parameter
Subscripts	
l	liquid
m	gas mixture
sat	saturated
sp	single-phase
tp	two-phase
v	vapor

1. INTRODUCTION

The use of clean-fuel and pollutant-free PEFCs, which convert chemical energy released during the electrochemical reaction of hydrogen and oxygen directly into electricity, still has substantial momentum for future sustainable and renewable energy conversion systems. The PEFC has become the most suitable fuel cell type for automotive as well as some portable applications. There is also a potential for back-up power unit applications, because of its low operating temperature, high power density and comparative simplicity of construction. The principle on which the fuel cell technology is based dates back to 1838 [1]. In spite of engineering progress and scientific advances over the last decades, the PEFC commercialization remains unrealized, mainly due to: (1) high prices of components and materials; (2) technical issues relating mainly to water management; (3) the membrane fragility; as well as (4) membrane hydration issues.

A typical flow field consists of a series of minichannels and ribs. The continuous removal of liquid water from the cathode channels of PEFC is a critical issue. On one hand, a perfect amount of water is required in PEFCs, for example, for membrane hydration. On the other hand, large water droplets formed in the channels, can cause flooding, i.e., blocking the transport of oxygen to the active sites. This causes not only a substantial loss of performance but also an uneven current distribution, unstable operation and enhanced degradation. Liquid water might break through at preferential locations to form droplets at the gas diffusion layer (GDL)/gas channel interface. When the momentum of the gas channel overcomes the droplet pinning force, the droplets will de-pin and be removed via one or more of the following three flow patterns: droplet flow (also called mist flow), film flow (also called annular flow) and slug flow. Flow pattern maps and pressure drop correlations of two-phase flow in micro/minichannels [2-4] might not be applicable for gas channels due to the one-side porous wall and the interaction between the GDL and the gas channel.

The flow and hydrodynamics in gas channels are important to maintain a delicate water balance. This work will focus on the frictional pressure drop in gas channels, which is of relevance for the reactant pumping power and the cell performance. Single-phase pressure drop in micro/minichannels is well understood and predictive methods for conventional channels are still applicable for micro/minichannels if the surface roughness and entrance effects are correctly realized [5]. However, the pressure drop prediction for two-phase flow is more complex and pressure drop correlations for conventional channels are not applicable any more, or only applicable within a limited range. Compared to adiabatic gas-liquid two-phase flow in microchannels, the two-phase flow in gas channels of PEFCs has its special features: (1) combination of reactant gas, water vapor and liquid water, (2) reactant consumption, (3) water vapor condensation, (4) continuous water introduction from reaction and (5) flow pattern transitions. As pressure drop for two-phase flow is closely coupled with flow patterns, flow-pattern based methods need to be developed to provide a relatively general and reliable prediction.

2. FLOW PATTERNS IN GAS CHANNELS

Due to continuous water introduction from the GDLs and possible water condensation from water vapor, the flow in gas channels may experience different flow patterns, e.g., single-phase gas flow, droplet flow or mist flow, film flow and slug flow. In the droplet/mist flow, small water droplets flow at the same velocity as the gas flow. The film flow indicates that liquid flows on the channel walls and gas flows in the core. The slug flow means large liquid plugs (longer than the channel diameter) with large gas slugs in between. Several in-situ experiments were performed to visualize two-phase flow patterns in operating fuel cells [6-8]. Hussaini and Wang [6] firstly observed all these flow patterns in an operating fuel cell and developed a flow pattern map. In this work, the flow pattern map of Hussaini and Wang [6], which can also capture the experimental data of See [7], is used to determine the flow patterns. It should be noted that within a PEFC, the microchannels have three solid walls and one porous wall (the gas channel/GDL interface) with significant different wall characteristics.

3. PRESSURE DROP MODELLING

In gas channels, liquid water emerges when the partial vapor pressure reaches the local saturation pressure corresponding to the local temperature. The local saturation pressure of the water component is given as [7]:

$$P_{\mathrm{sat,H2O}}(T) = -2846.4 + 411.24(T-273.15) - 10.554(T-273.15)^2 + 0.16636(T-273.15)^3 \qquad (1)$$

The partial vapor pressure can be obtained from the mole fraction of the water vapor:

$$\frac{P_{\mathrm{H2O}}}{P} = \frac{n_{\mathrm{H2O}}}{n} \qquad (2)$$

The relative humidity of the gas mixture (RH) is calculated as the ratio of the partial vapor pressure to the local saturation pressure:

$$\mathrm{RH} = \frac{P_{\mathrm{H2O}}}{P_{sat,\mathrm{H2O}}(T)} \qquad (3)$$

Assuming local thermodynamic equilibrium, three might be a single-phase flow zone (RH < 1) and a two-phase flow zone in gas channels, as shown in Fig. 1. If the relative humidity at the inlet of the gas channel is less than 100%, continuous water vapor from the GDL increases the partial vapor pressure and thus the relative humidity increases. When the partial vapor pressure equals to the local saturation pressure (i.e, RH = 1), liquid water emerges from the GDL and accumulates in the gas channel, leading to the gas mixture-liquid water two-phase flow zone. In other words, sub-saturated air (a gas mixture of air and water vapor) flows in the single-phase flow zone; while saturated air and liquid water exist in the two-phase flow zone.

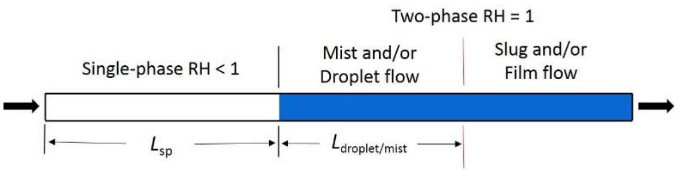

Fig. 1 Possible flow regimes in gas channels.

3.1 Superficial velocities for liquid water and the gas mixture

If we assume a uniform current distribution of the fuel cell, water is uniformly introduced into the gas channel. As shown in Fig. 2, when water injection is uniform along the gas channel, the superficial velocity of liquid water increases linearly along the gas channel in the two-phase flow zone.

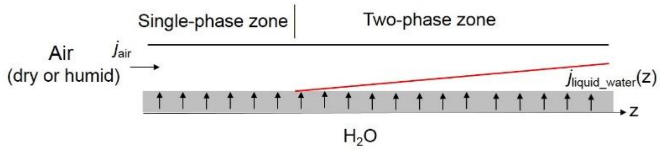

Fig. 2 Uniform water introduction into the gas channel.

Based on the Faraday's law, at a given current density the mass flow rate of air is [6]

$$\dot{m}_{air} = 2.38 \cdot \zeta \cdot M_{air} \cdot \frac{i \cdot A_{em}}{2F} \tag{4}$$

where ζ refers to the stoichiometry which indicates the ratio of the supplied air to the needed air (oxygen) for reaction. The mass flow rate of the consumed oxygen is [6]

$$\dot{m}_{O2} = M_{O2} \cdot \frac{i \cdot A_{em}}{4F} \tag{5}$$

The mass flow rate of water is [6]

$$\dot{m}_{\mathrm{H2O}} = \dot{m}_{\mathrm{H2O},v} + \dot{m}_{\mathrm{H2O},l} = (1 + 2\beta) \cdot M_{\mathrm{H2O}} \cdot \frac{i \cdot A_{em}}{2F} \tag{6}$$

As shown in Fig. 2, the superficial velocity of liquid water at the channel exit is given as

$$j_{\mathrm{H2O},l}(z = L) = \frac{L_{tp}}{L} \cdot \frac{\dot{m}_{\mathrm{H2O}}}{N \cdot A_c \cdot \rho_{\mathrm{H2O},l}} \tag{7}$$

Therefore, the superficial velocity of liquid water along the channel can be calculated as follows:

$$j_{\mathrm{H2O},l}(z) = \begin{cases} 0, & z < L_{sp} \\ \frac{1}{L} \cdot \frac{\dot{m}_{\mathrm{H2O}}}{N \cdot A_c \cdot \rho_{\mathrm{H2O},l}} (z - L_{sp}), & z \geq L_{sp} \end{cases} \tag{8}$$

The superficial velocity of the gas mixture can be obtained from the inlet mass flow rate of air, the oxygen consumption along the gas channel and the water vapor introduction during the single-phase flow zone. For simplicity, the oxygen consumption and the water vapor introduction can be neglected for calculation of the superficial velocity of the gas mixture. On one hand, the oxygen consumption and the water vapor introduction nearly cancel out each other in the single-phase flow zone. On the other hand, the ratio of the consumed air to the inlet supply air is relatively small considering the gas stoichiometry and the fraction of oxygen in air. Therefore, the superficial velocity of the gas mixture is given as

$$j_m = \frac{\dot{m}_{air}}{N \cdot A_c \cdot \rho_m} \tag{9}$$

3.2 Single-phase flow zone

For the single-phase flow zone where the relatively humidity (RH) is less than unity, the pressure drop can be calculated as follows:

$$\left(\frac{dP}{dz}\right)_{sp} = \frac{2fG^2}{\rho_m D_h} = fRe \frac{2\mu_m G}{D_h^2} \tag{10}$$

where *f*Re is given by Hartnett and Kostic [9], as listed below

$$fRe = 24(1 - 1.3553\alpha + 1.9467\alpha^2 - 1.7012\alpha^3 + 0.9564\alpha^4 - 0.2537\alpha^5) \tag{11}$$

The aspect ratio α is defined as the height divided by the width of the channel cross-section.

For humid air under-saturated with water vapor, the density of the gas mixture can be calculated by [10]

$$\rho_m = \frac{1}{Z(P_{\mathrm{H2O}}, T)} \frac{P}{R \cdot T} \cdot M_{air} \cdot \left[1 - E(P,T) \cdot \mathrm{RH} \cdot \left(1 - \frac{M_{\mathrm{H2O}}}{M_{air}}\right) \cdot \frac{P_{sat,\mathrm{H2O}}(T)}{P}\right] \tag{12}$$

where *Z* and *E* indicate the compressibility factor and the enhancement factor, respectively. The compressibility and enhancement factors can be fixed as unity with an error less than 1.0% for temperatures ranging from 0 to 80 ˚C. The viscosity of the gas mixture (humid air undersaturated with water vapor) can be calculated by [10]

$$\mu_m = \frac{\left[1 - E(P,T) \cdot RH \cdot \frac{P_{sat,\mathrm{H2O}}(T)}{P}\right] \cdot \mu_{air}}{\left[1 - E(P,T) \cdot RH \cdot \frac{P_{sat,\mathrm{H2O}}(T)}{P}\right] + E(P,T) \cdot RH \cdot \frac{P_{sat,\mathrm{H2O}}(T)}{P} \cdot \omega_{air,\mathrm{H2O}}} + \frac{E(P,T) \cdot RH \cdot \frac{P_{sat,\mathrm{H2O}}(T)}{P} \cdot \mu_{\mathrm{H2O},v}}{E(P,T) \cdot RH \cdot \frac{P_{sat,\mathrm{H2O}}(T)}{P} + \left[1 - E(P,T) \cdot RH \cdot \frac{P_{sat,\mathrm{H2O}}(T)}{P}\right] \cdot \omega_{\mathrm{H2O},air}} \tag{13}$$

where the interaction parameters $\omega_{\mathrm{air,H2O}}$ and $\omega_{\mathrm{H2O,air}}$ are given by [10]

$$\omega_{air,\mathrm{H2O}} = \frac{\sqrt{2}}{4}\cdot\left(1+\frac{M_{air}}{M_{\mathrm{H2O}}}\right)^{-\frac{1}{2}}\cdot\left[1+\left(\frac{\mu_{air}}{\mu_{\mathrm{H2O},v}}\right)^{\frac{1}{2}}\cdot\left(\frac{M_{\mathrm{H2O}}}{M_{air}}\right)^{\frac{1}{4}}\right]^2 \tag{14}$$

$$\omega_{\mathrm{H2O},air} = \frac{\sqrt{2}}{4}\cdot\left(1+\frac{M_{\mathrm{H2O}}}{M_{air}}\right)^{-\frac{1}{2}}\cdot\left[1+\left(\frac{\mu_{\mathrm{H2O},v}}{\mu_{air}}\right)^{\frac{1}{2}}\cdot\left(\frac{M_{air}}{M_{\mathrm{H2O}}}\right)^{\frac{1}{4}}\right]^2 \tag{15}$$

The molar mass of dry air, M_{air}, is 28.9635 kg/kmol. The viscosity of dry air is calculated by the following equation [11]

$$\mu_{air}\cdot 10^6 = -0.98601 + 9.080125\cdot 10^{-2}\cdot T - 1.17635575\cdot 10^{-4}\cdot T^2 + 1.2349703\cdot 10^{-7}\cdot T^3 - 5.7971299\cdot 10^{-11}\cdot T^4 \tag{16}$$

The viscosity of water vapor can be obtained by the following equation [12]

$$\mu_{\mathrm{H2O}}\cdot 10^6 = 80.58131868 + 0.4000549451\cdot T \tag{17}$$

During the single-phase flow zone, as discussed above, oxygen is consumed from the gas mixture while water is added into the gas mixture in the form of water vapor. The mass flow rate of the consumed oxygen is almost equal to the mass flow rate of the generated water vapor. Therefore, the total mass flow rate of the gas mixture can be assumed constant. The frictional pressure drop of the single-phase flow zone can be obtained by integrating Eq. (10) from $z = 0$ to $z = L_{\mathrm{sp}}$.

3.3 Two-phase flow zone

There are two concepts for two-phase frictional pressure drop modelling: homogeneous flow modelling and separated flow modelling. In the homogeneous flow modelling, the two-phase mixture is assumed as a pseudo single-phase flow by using averaged viscosity and density values. In the droplet/mist flow pattern in gas channels of PEFCs, the small droplets flow at the same velocity as the gas mixture, i.e., zero slip velocity. Therefore, the homogeneous model can be used to calculate the frictional pressure drop in the droplet/mist flow

$$\left(\frac{dP}{dz}\right)_{droplet/mist} = \frac{2f_{tp}G^2}{\rho_{tp}D_h} = (fRe)_{droplet/mist}\frac{2\mu_{tp}G}{\rho_{tp}D_h^2} \tag{18}$$

where $(fRe)_{droplet/mist}$ can be obtained from Eq. (11). The average density is given by

$$\rho_{tp} = \left(\frac{x}{\rho_m}+\frac{1-x}{\rho_{\mathrm{H2O},l}}\right) \tag{19}$$

There are different two-phase viscosity models. Different viscosity models might give a large difference in prediction of the frictional pressure drop [4]. The Dukler et al. [13] model is used in the present method, which shows good accuracy for the droplet/mist flow

$$\mu_{tp} = \rho_{tp}\left[\frac{x\cdot\mu_m}{\rho_m}+\frac{(1-x)\cdot\mu_{\mathrm{H2O},l}}{\rho_{\mathrm{H2O},l}}\right] \tag{20}$$

The frictional pressure drop of the droplet/mist flow regime can be obtained by integrating Eq. (18) from $z = L_{\mathrm{sp}}$ to $z = L_{\mathrm{sp}} + L_{\mathrm{droplet/mist}}$, where $L_{\mathrm{droplet/mist}}$ is the length of the droplet/mist flow regime.

For slug flow and film flow patterns, as there is a slip between the liquid phase and the gas phase, separated flow models are preferred to homogeneous flow models to calculate the frictional pressure drop of the slug flow. In the separated flow model, the two-phase frictional pressure drop is estimated based on the pressure drop of one phase multiplied by the two-phase frictional multiplier [14]

$$\left(\frac{dP}{dz}\right)_{slug/film} = \phi_m^2\left(\frac{dP}{dz}\right)_m = (1 + C\cdot X + X^2)\left(\frac{dP}{dz}\right)_m \tag{21}$$

$$\left(\frac{dP}{dz}\right)_{\mathrm{H2O},l} = (fRe)_{\mathrm{H2O},l}\frac{2\cdot\mu_{\mathrm{H2O},l}\cdot j_{\mathrm{H2O},l}}{D_h^2} \tag{22}$$

$$\left(\frac{dP}{dz}\right)_m = (fRe)_m\frac{2\cdot\mu_m\cdot j_m}{D_h^2} \tag{23}$$

where X is the Martinelli parameter

$$X^2 = \frac{(dP/dz)_{\mathrm{H2O},l}}{(dP/dz)_m} \tag{24}$$

The Martinelli parameter can be simplified if both the gas and liquid flows in the gas channels are laminar:

$$X^2 = \frac{\mu_{\mathrm{H2O},l}\cdot j_{\mathrm{H2O},l}}{\mu_m\cdot j_m} \tag{25}$$

The frictional pressure drop of the droplet/mist flow regime can be obtained by integrating Eq. (21) from $z = L_{\mathrm{sp}} + L_{\mathrm{droplet/mist}}$ to $z = L$.

Finally, the total frictional pressure drop can be calculated by the following equation

$$\Delta P_{total} = \Delta P_{sp} + \Delta P_{droplet/mist} + \Delta P_{slug/film} \tag{26}$$

The values of the three terms on the right-hand side of the above equation depend on the operating and flowing conditions. For example, if the air is still not saturated at the end of the gas channel, then the last two terms on the right-hand side are zero. If the air is saturated at the channel inlet, the first term of the right-hand side is probably zero. If slug and/or film flow patterns do not exist in the two-phase flow zone, the last term is zero.

Therefore, a flow-pattern based pressure drop model is proposed in this section. Firstly, the single-phase and two-phase flow zones in the gas channel are identified by evaluating the value of relative humidity. Secondly, flow patterns in the two-phase flow zone are identified by the Hussaini and Wang [6] flow pattern map based on the superficial velocities of liquid water and the gas mixture. Then, specific to gas channels in PEFCs, different models need to be used for subsections of different flow regimes, e.g., single-phase correlations for gas flow, homogeneous flow models for droplet/mist flow and separated flow models for film and slug flow patterns. Property variations might be neglected for small temperature differences. Besides, each flow regime might be segmented into several control volumes considering the variation of the water introduction along the length of the gas channels, i.e., the variations of the liquid and gas superficial velocities.

4. COMPARISONS WITH LITERATURE DATA

In this section, the total frictional pressure drop calculated by the above model will be compared with literature data and possible modifications of the Chisholm parameter *C* might be realized for better pressure drop estimations.

There are very limited pressure drop data for operating PEFCs in the literature. Two data sets are selected: Anderson et al. [15] and See [7] as these two data sets are for operating fuel cells with corresponding flow pattern information. For these two data sets, all the parameters needed in this modelling are given, including the inlet RH, air stoichiometry, current density, active membrane area, inlet temperature and pressure, flow field, channel dimensions and the measured pressure drop. Besides, the minor pressure losses are deduced from the measured pressure drop to get the total frictional pressure drop.

Figure 3 compared the estimated pressure drop by the present model with experimental data for a non-operating PEFC [15]. On one hand, it is not surprising that the experimental data are predicted very well as there is only single-phase gas flowing in the channel without any liquid water. On the other hand, the agreement suggests that the mixture properties, such as the mixture viscosity can be calculated by the equations in Section 3.2.

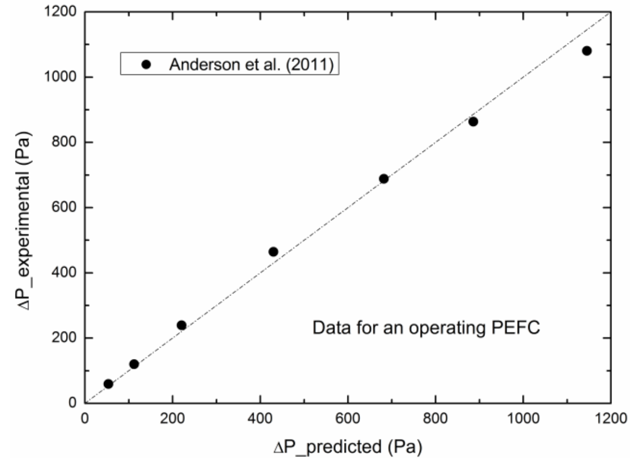

Fig. 3 Comparison of the present model with experimental data of Anderson et al. [15] for single-phase gas flow.

Figure 4 shows the predictive ability of the developed predictive method for droplet/mist flow by using experimental data of See [7]. The flow regime for the selected data points in Fig. 4 is droplet/mist flow. For those data points, the inlet air is saturated (RH = 1). Besides, according to the flow pattern map of Hussain and Wang [6] together with the flow pattern information provided in See [7], the flow regime is still droplet flow under the corresponding flow conditions. In this droplet/mist flow regime, the homogeneous flow modelling is adopted. As shown in Fig. 4, the present model can estimate the pressure drop in the droplet/mist flow regime relatively well, although it tends to under-predict the experimental data slightly.

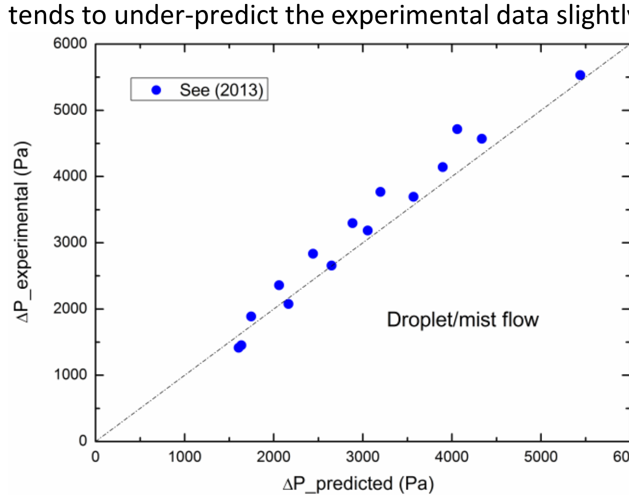

Fig. 4 Comparison of the present model with experimental data of See [7] for droplet/mist flow.

From Figs. 3 and 4, the pressure drops in the single-phase flow zone and the droplet/mist flow regime can be predicted relatively well. The pressure drop modelling in the slug/film flow regime is not as straightforward as those in the single-phase flow zone and the droplet/mist flow regime. The separated flow modelling should be adopted to model the frictional pressure drop in the slug/film flow regime. Various modifications of the Chisholm parameter *C* were presented in the literature to match the experimental data. For example, the value of the original Chisholm parameter for laminar gas and laminar liquid two-phase flow is 5.

For the two data sets of Anderson et al. [15] and See [7], it is found that a *C* value of 8.5 can predict the frictional pressure drops in the slug/film flow regime very well. Therefore, the following correlation is proposed for the slug/film flow regime to complete the flow-pattern based pressure drop modelling.

$$C = 8.5 \pm 0.5 \quad (27)$$

The modified *C* is higher than the original *C* = 5 for laminar air and laminar liquid water two-phase flow. The possible reasons might be the differences in the bounding walls and the introduction of air and liquid water. In PEFCs, the gas channel is comprised of three rigid walls and a porous wall. The porous wall might present more friction on the fluid flow than the rigid smooth wall. Besides, *C* = 5 was originally proposed assuming that air and liquid water are introduced simultaneously from the inlet. However, for PEFCs, liquid water is introduced into the gas channel from a porous wall, which might introduce some additional disturbances and increase the fluid friction. Figure 5 shows that the modified *C*, combining with the homogeneous flow modelling, can estimate the pressure drop values in the two-phase flow zone relatively well.

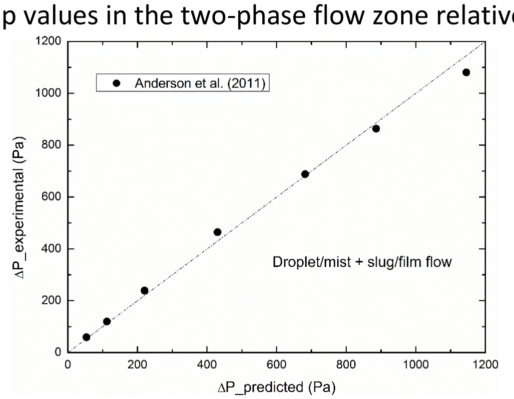

(a)

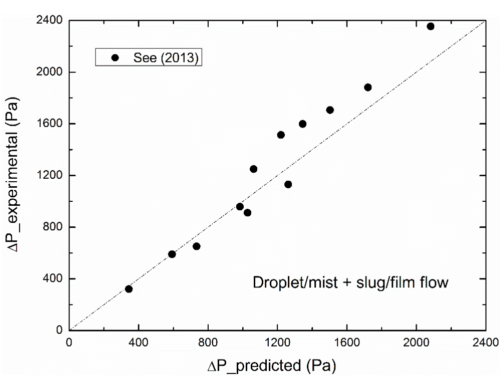

(b)

Fig. 5 Comparison of the present model with experimental data of (a) Anderson et al. [15] and (b) See [7] for droplet/mist and slug/film flow regimes.

5. CONCLUSIONS

A flow-pattern based pressure drop model has been proposed for predicting the frictional pressure drop in gas channels of PEFCs. Overall, the new model can estimate the data of Anderson et al. [19] and See [10] well, predicting most of the data points within a ± 10% error band. The relative humidity was used to classify the single-phase flow zone from the two-phase flow zone. In the droplet/mist flow regime of the two-phase flow zone, a homogeneous flow modelling was adopted, while in the slug/film flow regime of the two-phase flow zone, a modified Chisholm value of 8.5 was used. Previous pressure drop correlations for adiabatic air-water two-phase flow may not be applicable for gas channels in PEFCs due to the one-side porous wall and the interaction between the GDL and the gas channel.

The flow-pattern specific model needs more validation as there are very limited pressure drop and flow pattern measurements for operating PEFCs in the literature.

REFERENCE

[1] Schönbein, C., (1838) Further experiments on the current electricity excited by chemical tendencies, independent of ordinary chemical action, *Lond. Edinb. Philos. Magaz. J. Sci.*, 12, 311-317.

[2] Ullmann, A., & Brauner, N. (2007). The prediction of flow pattern maps in minichannels. *Multiphase Science and Technology*, *19*(1), 49-73.

[3] Kawahara, A., Sadatomi, M., Nei, K., & Matsuo, H. (2009). Experimental study on bubble velocity, void fraction and pressure drop for gas-liquid two-phase flow in a circular microchannel. *International Journal of Heat and Fluid Flow*, *30*(5), 831-841.

[4] Li, W., & Wu, Z. (2010). A general correlation for adiabatic two-phase pressure drop in micro/mini-channels. *International Journal of Heat and Mass Transfer*, *53*(13), 2732-2739.

[5] Wu, Z., & Sundén, B. (2014). On further enhancement of single-phase and flow boiling heat transfer in micro/minichannels. *Renewable and Sustainable Energy Reviews*, *40*, 11-27.

[6] Hussaini, I. S., & Wang, C. Y. (2009). Visualization and quantification of cathode channel flooding in PEM fuel cells. *Journal of Power Sources*, *187*(2), 444-451.

[7] See, E. (2013). In situ measurement, characterization, and modeling of two-phase pressure drop incorporating

local water saturation in PEMFC gas channels. M.S. thesis, Rochester Institute of Technology, Troy, NY.
[8] Banerjee, R., & Kandlikar, S. G. (2014). Liquid water quantification in the cathode side gas channels of a proton exchange membrane fuel cell through two-phase flow visualization. *Journal of Power Sources*, *247*, 9-19.
[9] Hartnett, J. P., & Kostic, M. (1989). Heat transfer to Newtonian and non-Newtonian fluids in rectangular ducts. *Advances in Heat Transfer*, *19*, 247-356.
[10] Tsilingiris, P. T. (2008). Thermophysical and transport properties of humid air at temperature range between 0 and 100 C. *Energy Conversion and Management*, *49*(5), 1098-1110.
[11] Irvine, T. F., & Liley, P. E. (1984). *Steam and gas tables with computer equations* (Vol. 1983). Academic Press.
[12] Touloukian, Y. S. (Ed.). (1970). *Thermophysical Properties of Matter: Viscosity, by YS Touloukian, SC Saxena, and P. Hestermans* (Vol. 11). Ifi/Plenum.
[13] Dukler, A. E., Wicks, M., & Cleveland, R. G. (1964). Frictional pressure drop in two-phase flow: B. An approach through similarity analysis. *AIChE Journal*, *10*(1), 44-51.
[14] Chisholm, D. (1967). A theoretical basis for the Lockhart-Martinelli correlation for two-phase flow. *International Journal of Heat and Mass Transfer*, *10*(12), 1767-1778.
[15] Anderson, R., Wilkinson, D. P., Bi, X., & Zhang, L. (2011). Two-phase flow pressure drop hysteresis in an operating proton exchange membrane fuel cell. *Journal of Power Sources*, *196*(19), 8031-8040.